Online ISSN 1848-3380, Print ISSN 0005-1144
ATKAFF 57(1), 188–200(2016)

Abdullah Bajelan, Adel Akbarimajd

A New Mechanism for Passive Dynamic Object Manipulation along a Curved Path

DOI 10.7305/automatika.2016.07.818
UDK 621.865.8-229.31:681.532; 517.93

Original scientific paper

Object manipulation is a basic task in robotics and automation. Active manipulation by grasp is conventional approach in object manipulation. However, in many cases, grasp-less manipulation can be beneficial in terms of cost, minimalism and extension of workspace. On the other hand passive mechanisms are advantageous from the energy saving viewpoint. In this paper we combine these ideas to develop a dynamic passive object manipulation mechanism to achieve manipulation in more than one dimension and simultaneously change position and orientation of the object. In developed mechanism the manipulation platform is a simple inclined surface. The object is composed of two wheels with different radiuses and an axle connecting the wheels to each other. The object moves passively along a circular path on the platform. Kinematic equations of the motion are devised, dynamic analyses are performed and no-slippage conditions are extracted. Modelling in CATIA and simulations in MSC.ADAMS are performed and experimental set up is built to verify the analysis.

Key words: Dynamics, Grasp-less manipulation, Object manipulation, passive mechanism

Novi mehanizam za pasivno-dinamičnu manipulaciju objektom duž zakrivljenog puta. Manipulacija objektom je osnovni zadatak u robotici i automatici. Aktivna manipulacija hvatom predstavlja konvencionalan prostup manipulaciji objektom. Ipak, u mnogim slučajevima, manipulacija objektom bez hvata može biti korisna u smislu troškova, minimalizma i proširenja radnom prostora. S druge strane, pasivni mehanizmi posjeduju prednosti iz perspektive uštede energije. U ovom radu mi kombiniramo ove ideje kako bismo razvili dinamično-pasivni mehanizam za manipulaciju objektom u svrhu postizanja manipulacije u više od jedne dimenzije i simultano mijenjali poziciju i orijentaciju objekta. U razvijenom mehanizmu platforma za manipulaciju sastoji se od jednostavne nagnute plohe. Objekt se sastoji od dvaju kotača različitih radijusa i jedne osi koja spaja kotače. Objekt se kreće pasivno duž zakrivljenog puta na platformi. Postaljene su jednadžbe kinematike gibanja, te je analizirana dinamika, dok je klizanje zanemareno. U svrhu verifikacije analize izrađen je model eksperimentalnog postava u CATIA-i te su provedene simulacije korištenjem MSC.ADAMS alata.

Ključne riječi: Dinamika, manipulacija bez hvata, manipulacija objektom, pasivni mehanizam

1 INTRODUCTION

Object manipulation is an essential task in industries. The object manipulation can be a part of a complicated task such as painting, welding, assembly etc. [1] or it can be desirable by itself (ex [3]). As three familiar examples we can refer to:

1. A set of conveyors carry a part from one position to other one as well as changing its orientation (Fig 1.). Programming of system is a challenge [6].

2. Wagons in mines move articles from one configuration to other one (Fig 1.). Kinematic and dynamical analysis are some challenges [7].

3. A robotic arm changes position and orientation of the object (Fig 1.). Stable grasp and task space planning are some challenges [8]-[10].

In all above examples an object is manipulated from one configuration to another one.

In the literature, two categories of object manipulation techniques can be recognized: manipulation with grasp and manipulation without grasp. In manipulation with grasp, the object is held by robot hand and then it is moved to goal configuration. Some relevant recent researches can be found in [11]-[14]. In grasp-less manipulation (or nonprehensile manipulation), the object is manipulated by manoeuvres like pushing [15][16], pivoting [17], sliding [18], juggling [19]-[22], translation and rotation [23],

[24] etc. Grasp-less manipulation approach has some advantages and some disadvantages over manipulation with grasp. Advantages of grasp-less manipulation include minimalism in mechanism [25], reduction in cost [26], opportunity of transferring object out of robot's workspace [19], [20], elimination of need for compliance control and finger coordination in establishing stable grasp, possibility of doing tasks with more DoF (Degrees of Freedom) than the DoF of the robot [27] and exploiting geometry and dynamics of the environment in performing the manipulation [25]. When different tasks are not expected from the mechanism, manipulation task is not complicated and simplicity and cost are most important factors, grasp-less manipulation is preferred.

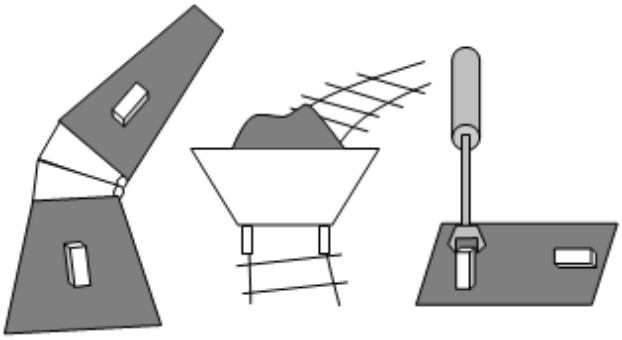

Fig. 1. Three examples of object manipulation in industries. The set of conveyors is given on the left, the wagon on rail in the middle and robotic arm on the right. In most of cases both position and orientation of the object should be changed.

Fig. 2. Sliding of penguins and rolling of hedgehog are passive manipulation examples in nature.

As a matter of fact, grasp-less manipulation is the most common approach in the nature. One can hardly find grasp when object are being manipulated in nature. There is another manipulation approach in nature that leads to energy saving mechanisms and simpler systems. That is passive manipulation which means manipulation without actuator and active controllers. Flowing the river down the mountains to the sea, rolling hedgehog down hills and sliding penguins on the ice are some interesting examples of passive grasp-less manipulation in nature (see Fig. 2).

The idea of using passive mechanisms in robotics has been probably initiated by works of McGeer (Fig. 3) where he inspired from rotation of rimless wagon wheel to design his passive dynamic walkers [28].

Since then a lot of works have been reported in the field of passive locomotion. One can find some examples in [29]-[35]. As it was shown that locomotion is dynamically analogous to manipulation [24], [36], [37], the results of studies on passive locomotion can be utilized in design of

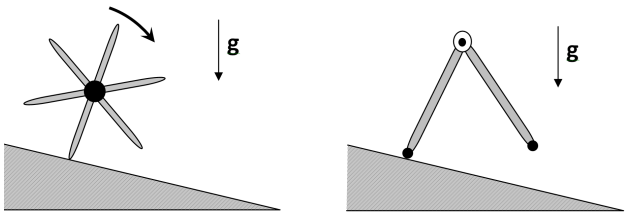

Fig. 3. McGeer inspired from passive motion of rimless wheel to develop passive dynamic walker. that became basis of many researches in passive dynamics.

passive locomotion mechanisms. The idea of passive manipulation, however, was firstly introduced in [38] where four significant properties of passive manipulation were introduced and three examples were presented.

In passive locomotion and passive manipulation mechanisms, the only motion generation force is gravity and there is no active controller. More specifically, in these mechanisms there is an inclined plane which acts as a tool to exploit gravity force for motion generation.

It is well-known that the configuration of an object is defined by six components (three position components and three orientation components). In existing works of passive mechanisms, the generated motion is always along a straight line. However, in many manipulation applications more than one component has to be changed. Straight line manipulation only changes one position component, therefore it is not desired. In many applied cases a curved path is required which means more than one-dimensional manipulation. In the literature, no passive mechanism has been reported for manipulation on curved path. In such a mechanism, a structural intelligence is required to guide the object on a computable curved path. Such a manipulation mechanism should be capable of simultaneously changing position and orientation of the object.

In this paper we combine ideas of grasp-less manipulation and passive manipulation to introduce a mechanism for object manipulation along a curved path. The path can be specified according to kinematic and dynamical parameters of the object and the mechanism. The mechanism is simple and advantageous from energy saving viewpoint as it does not need external actuation.

This paper is extension of our previously presented conference paper [39]. In that work only kinematic analysis of the mechanism was presented with no experimental justification. In this paper dynamical analysis, some potential applications of the mechanism, experimental verification and studies on the effect of the model parameters on the motion are provided.

2 PROBLEM DEFINITION

The aim of this paper is to develop a mechanism for grasp-less passive manipulation of an object along a planned curved path. The mechanism consists of two components. The first component is the manipulated object and the second one is platform wherein the object is manipulated. The platform is in dynamic interaction with the object and their geometry and dynamics determine the motion parameters of the object.

Simultaneous design of the object and the platform can be complicated and in most cases it is not necessary. Here, one may have two approaches to this problem. The first approach is to choose a simple object and design the platform and the second approach is to choose a simple platform and design the object. The researches published in this filed have adopted the second approach while the first approach can also be valuable in some cases. This paper takes the second approach for the first time. Besides providing passive dynamic manipulation on a computable curved path - that was explained earlier in Introduction - taking this approach to the problem is another contribution of the paper.

In our proposed mechanism, the platform is considered to be a simple inclined surface with slope β_0 as it is shown in Fig. 4. Then, we should design the object in such a way that it can travel on a determined curved route. The proposed object, as it is shown in Fig. 4, is composed of a pair of wheels with different radiuses those are connected together by an axle. In the rest of this paper we refer to this setup as *object*. Masses of the small and big wheels are assumed to be m_{ws} and m_{wb} respectively and mass of the axle is neglected; then total mass of the object will be $M' = m_{ws} + m_{wb}$. The radius of the small and big wheels are assumed to be r_{ws} and r_{wb} respectively (see Fig. 4). The axle is connected to the center point of interior surfaces of wheels and length of its projection on the surface is L_0. Width of wheels is b and the radius of axle is r_{ro}.

Without loss of generality, it is assumed that in initial configuration, the axle is located perpendicular to the gradient of the ramp as it is shown in Fig. 5.

The aim of this paper is to analyze kinematics and dynamics of motion of the object and obtain travelled path and motion equations. We assume that there is no slippage and the motion is perfect rolling. Obviously the motion and path will be related to parameters of the object

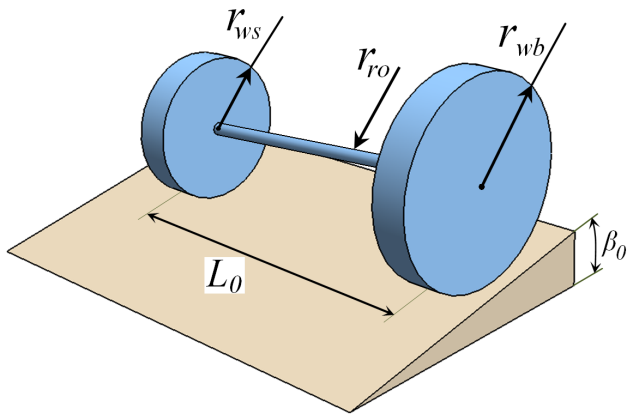

Fig. 4. The proposed mechanism. A simple inclined surface with slope β_0 and an object composed of two wheels with different radiuses.

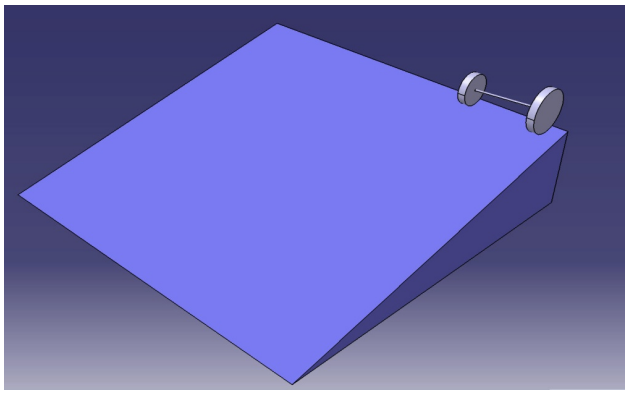

Fig. 5. Initial condition of the mechanism where axle of the object is located perpendicular to gradient of the ramp.

and slop of the platform. Then motion and path planning of the object can be achieved by appropriately selection of the parameters of the mechanism. In the rest of paper we will address these points in more details. Section 3 includes kinematics analysis of the motion. This section is summary of [38] which is our work preliminary to this paper. In fourth section dynamical analysis is provided and in Section 5 no-slippage condition is devised. Section 6 includes simulation and experimental results and the finally last section concludes the paper and provides the idea of the way that the proposed mechanism may be used in applied manipulation systems.

3 KINEMATICAL MODEL OF PROPOSED MECHANISM

Fig. 6 shows free body diagram of the object at starting time of the motion. To study motion of the object, we considered right handed coordinates frame O_{XYZ} for the

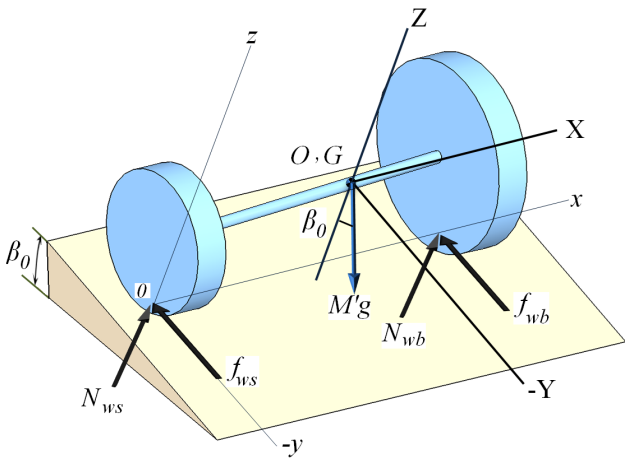

Fig. 6. Free body diagram of the proposed mechanism at the starting time of the motion.

object in such a way that its origin O is located in the object Center of Gravity (CoG), X axis is parallel with the projection of center to center distance of wheels on the platform and Z axis is normal to the surface. This frame which we call it "*path-based frame*", moves with the object. Another frame o_{xyz} is considered parallel to O_{XYZ} such that its origin o is located at the bottom of the smaller wheel. Coordinates of object's CoG in o_{xyz} is given by $(\bar{x}, \bar{y}, \bar{z})$. $N_{ws}$and N_{wb} are normal forces applied from the surface to the wheels and f_{ws} and f_{wb} are friction forces.

At each time instance, we denote the linear velocity and acceleration of the object CoG in Y direction by v and a respectively. Apparently, different points of the object have different linear velocities in Y direction and the same angular velocity in X direction. Linear velocities of wheels CoG in y-direction are given as:

$$v_{ws} = \omega_x r_{ws} \Rightarrow a_{ws} = \dot{\omega}_x r_{ws} \tag{1}$$

$$v_{wb} = \omega_x r_{wb} \Rightarrow a_{wb} = \dot{\omega}_x r_{wb} \tag{2}$$

where ω_x denotes angular velocity of the object in x direction. From (1) and (2) we obtain:

$$\dot{\omega}_x = \frac{a_{ws}}{r_{ws}} = \frac{a_{wb}}{r_{wb}} \tag{3}$$

Let R be the radius of the circular path and Z_0 the axis of rotation of the object as it is shown in Fig. 6. Difference between linear velocities of the wheels CoG is invariable which results in a circular path for the object from the normal point of view of the surface. Obviously, taking in account the height change in moving down the slope, the object's path is a helix from the view point of a reference frame located in the level ground. Angular acceleration of

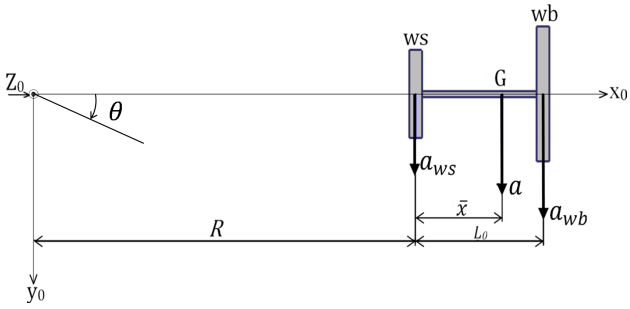

Fig. 7. Objects geometry and its accelerations from the normal point of view of the surface.

the object about Z_0 is given as:

$$\dot{\omega}_{Z_0} = -\frac{a}{R + \bar{x}} \tag{4}$$

where $\bar{x}$ is x-component of CoG of the object in o_{xyz}. Then we obtain linear accelerations of wheels CoG in terms of $\dot{\omega}_{Z_0}$as:

$$a_{ws} = \dot{\omega}_{Z_0} R = -\frac{a}{R + \bar{x}} R \tag{5}$$

$$a_{wb} = \dot{\omega}_{Z_0}(R + L_0) = -\frac{a}{R + \bar{x}}(R + L_0) \tag{6}$$

Substituting a_{ws} and a_{wb} from (5) and (6) in (3) we obtain radius of the path as:

$$R = \frac{r_{ws} L_0}{r_{wb} - r_{ws}} \tag{7}$$

4 DYNAMIC MODEL OF PROPOSED MECHANISM

In this section we obtain X, Y and Z components of accelerations of the object according to free body diagram of Fig. 6 and using kinematics equations of the previous section. To this end we firstly specify forces and torques applied to the object in the previously defined path-based frame. Then we obtain accelerations at different time steps in association with the applied torque and forces. We denote rotation of the object around Z_0 axis (see Fig. 7) by θ and we assume that at the beginning of the motion (state of Fig. 4 and 5) we have $\theta(t = 0) = 0$. If we consider motion in the path-based frame in our problem, different motion factors including torques, forces and accelerations will be determined by changes of θ.

In our analysis, to simplify the modelling, we neglect the centrifugal force in x direction applied from the surface to the object due to friction forces. We also neglect component of the weight of the object in x direction. It is worth mentioning that the magnitude and direction of the x-component of the weight varies and depends on angle θ.

From the starting angle $\theta = 0$ to angle $\theta = \frac{\pi}{2}$ above-mentioned x component of centrifugal force and weight component are in the opposite direction and their resultant effect is reduced. On the other hand in small values of slope β_0, above forces will be small. Then assuming small slopes and motion range of $0 < \theta < \frac{\pi}{2}$ neglecting of these forces is applicable. Before we obtain motion equations, let we find coordinates of object's CoG in o_{xyz} frame. We have:

$$\bar{x} = \frac{m_{ws}\bar{x}_{ws} + m_{wb}\bar{x}_{wb}}{M'} \tag{8}$$

where $\bar{x}_{ws}$ and $\bar{x}_{wb}$ are x-components of CoG of small and big wheels in o_{xyz} and we have $\bar{x}_{ws} = 0$ and $\bar{x}_{ws} = L_0$. Then (8) can be rewritten as:

$$\bar{x} = \frac{m_{wb}L_0}{M'} \tag{9}$$

In a similar way we write:

$$\bar{y} = \frac{m_{ws}\bar{y}_{ws} + m_{wb}\bar{y}_{wb}}{M'} \tag{10}$$

$$\bar{z} = \frac{m_{ws}\bar{z}_{ws} + m_{wb}\bar{z}_{wb}}{M'} \tag{11}$$

As for y and z components of CoG of object we have $\bar{y}_{ws} = \bar{y}_{wb} = 0$, $\bar{z}_{ws} = r_{ws}$ and $\bar{z}_{wb} = r_{wb}$, then we get:

$$\bar{y} = 0 \tag{12}$$

$$\bar{z} = \frac{m_{ws}r_{ws} + m_{wb}r_{wb}}{M'} \tag{13}$$

Now we can obtain motion equations. For the configuration of Fig. 6 we have:

$$\sum F_X = 0 \tag{14}$$

$$\sum F_Y = M'a \tag{15}$$

$$\sum F_Z = 0 \tag{16}$$

$$\sum M_X = \dot{H}_X - H_Y\omega_Z + H_Z\omega_Y \tag{17}$$

$$\sum M_Y = \dot{H}_Y - H_Z\omega_X + H_X\omega_Z \tag{18}$$

$$\sum M_Z = \dot{H}_Z - H_X\omega_Y + H_Y\omega_X \tag{19}$$

where $\omega_X, \omega_Y, \omega_Z$ are components of angular velocity about G (CoG of the object) and H_X, H_Y, H_Z are components of angular momentum about G. To solve motion equations (17) to (19) we should find time derivatives of angular momentum H. The components of H can be written as:

$$H_X = I_X\omega_X - I_{XY}\omega_Y - I_{XZ}\omega_Z \tag{20}$$

$$H_Y = -I_{YX}\omega_X + I_Y\omega_Y - I_{YZ}\omega_Z \tag{21}$$

$$H_Z = -I_{ZX}\omega_X - I_{ZY}\omega_Y + I_Z\omega_Z \tag{22}$$

where I denotes moment of inertia of the object. Different components of I are given as:

$$\begin{aligned} I_X = {} & \tfrac{1}{2}(m_{ws}r_{wb}^2 + m_{ws}r_{ws}^2) + m_{wb}(r_{wb} - \bar{z})^2 \\ & + m_{ws}(\bar{z} - r_{ws})^2 \end{aligned} \tag{23}$$

$$\begin{aligned} I_Y = {} & \tfrac{1}{12}\left(m_{wb}(3r_{wb}^2 + b^2) + m_{ws}(3r_{ws}^2 + b^2)\right) \\ & + m_{wb}\left((L_0 - \bar{x})^2 + (r_{wb} - \bar{z})^2\right) \\ & + m_{ws}\left(\bar{x}^2 + (\bar{z} - r_{ws})^2\right) \end{aligned} \tag{24}$$

$$\begin{aligned} I_Z = {} & \tfrac{1}{12}\left(m_{wb}(3r_{wb}^2 + b^2) + m_{ws}(3r_{ws}^2 + b^2)\right) \\ & + m_{wb}(L_0 - \bar{x})^2 + m_{ws}\bar{x}^2 \end{aligned} \tag{25}$$

$$I_{XY} = I_{ZY} = 0 \tag{26}$$

$$I_{XZ} = m_{wb}(L_0 - \bar{x})(r_{wb} - \bar{z}) + m_{ws}\bar{x}(\bar{z} - r_{ws}) \tag{27}$$

Details about obtaining above components are given in the appendix A. As O_{XYZ} frame moves with the object, then obtained moments and products of inertia are fixed in O_{XYZ} and their derivatives are zero. On the other hand, as the object roles on the surface parallel to Y, the components of moment, angular velocity and angular acceleration in y direction are zero:

$$\sum M_Y = 0 \tag{28}$$

$$\dot{\omega}_Y = 0 \tag{29}$$

$$\omega_Y = 0 \tag{30}$$

Consequently we can take time derivatives of angular momentum as:

$$\dot{H}_X = I_X\dot{\omega}_X - I_{XZ}\dot{\omega}_Z \tag{31}$$

$$\dot{H}_Y = 0 \tag{32}$$

$$\dot{H}_Z = -I_{ZX}\dot{\omega}_X + I_Z\dot{\omega}_Z \tag{33}$$

Regarding to the fact that angular velocity is a free vector we have:

$$\dot{\omega}_Z = \dot{\omega}_{Z_0} \tag{34}$$

$$\dot{\omega}_X = \dot{\omega}_x \tag{35}$$

Now to extract motion equations we use Newton rules to write three equations for $\sum F_Y$, $\sum M_X$ and $\sum M_Z$ as:

$$\sum F_Y : \ f_{wb} + f_{ws} - M'g\sin\beta_0\cos\theta = -M'a \tag{36}$$

$$\sum M_X : \ f_{wb}\bar{z} + f_{ws}\bar{z} = I_X\dot{\omega}_X - I_{XZ}\dot{\omega}_Z \tag{37}$$

$$\sum M_Z : \ f_{wb}(L_0 - \bar{x}) - f_{ws}\bar{x} = -I_{ZX}\dot{\omega}_X + I_Z\dot{\omega}_Z \tag{38}$$

Now we can find $\dot{\omega}_x$ from substituting (5) in (1) as:

$$\dot{\omega}_X = -\frac{a}{r_{ws}(R + \bar{x})}R \tag{39}$$

Substituting $\dot{\omega}_X$ and $\dot{\omega}_Z$ from (39) and (4) in (37), then finding $f_{wb} + f_{ws}$ yields:

$$f_{wb} + f_{ws} = \frac{a}{\bar{z}(R+\bar{x})}\left(I_{XZ} + \frac{I_X R}{r_{ws}}\right) \quad (40)$$

Finally, substituting (39) in (36) we get linear acceleration of the motion as:

$$a = \frac{(R+\bar{x})\bar{z}r_{ws}M'g\sin\beta_0\cos\theta}{I_{XZ}r_{ws} + I_X R + \bar{z}r_{ws}M'(R+\bar{x})} \quad (41)$$

Equation (41) shows that how the acceleration of the object depends the slop β_0, parameters of the object including mass *M'*, inertia *I* and position of CoG parameters and its rotation on the platform. Using acceleration of the object, we can find velocity and displacement equations and specify motion time. According to (41), by selecting different values for slop $\beta_0$and object geometry parameters r_{ws}, r_{wb} and L_0 (those specify $\bar{x}$ and $\bar{z}$) we can independently take control on three degrees of freedoms R, θ, *Z* in designing of mechanism. This means that a desired circular motion can be achieved by appropriate design of system parameters.

It is obvious that the object's angular accelerations are also changed during motion. The angular accelerations about z and x directions can be easily obtained by kinematics equations and using linear velocity of (41) as:

$$\dot{\omega}_Z = \frac{-\bar{z}r_{ws}M'g\sin\beta_0\cos\theta}{I_{XZ}r_{ws} + I_X R + \bar{z}r_{ws}M'(R+\bar{x})} \quad (42)$$

$$\dot{\omega}_X = \frac{\bar{z}RM'g\sin\beta_0\cos\theta}{I_{XZ}r_{ws} + I_X R + \bar{z}r_{ws}M'(R+\bar{x})} \quad (43)$$

The analysis of previous sections are valid if the motion is pure rolling without slippage. We can write no slippage conditions as the sequel:

$$f_{ws} \le \mu N_{ws} \quad (44)$$

$$f_{wb} \le \mu N_{wb} \quad (45)$$

where μ is Coulomb friction coefficient. Adding these equations we can write no-slippage condition as:

$$f_{ws} + f_{wb} \le \mu(N_{ws} + N_{wb}) \quad (46)$$

As the *z*-axis is normal to the surface of the platform and the object does not leave the surface, then it has no acceleration in *z*-direction, then we have:

$$\sum F_Z = 0 \quad \Rightarrow \quad N_{ws} + N_{wb} = M'g\cos\beta_0 \quad (47)$$

Then from (46) we have:

$$f_{ws} + f_{wb} \le \mu M'g\sin\beta_0 \quad (48)$$

Substituting $f_{ws} + f_{wb}$ from (48) in (40) we get:

$$\mu \ge \frac{(I_{XZ}r_{ws} + I_X R)\tan\beta_0\cos\theta}{I_{XZ}r_{ws} + I_X R + \bar{z}r_{ws}M'(R+\bar{x})} \quad (49)$$

5 SIMULATION AND EXPRIMENT

5.1 Model verification

In this sub-section, in order to evaluate correctness of the obtained model, we perform a comparative study between the model and simulation and experimental results. In simulations, as a basic test, we considered an object with wheels radiuses $r_{ws} = 30\text{mm}$, $r_{wb} = 37.5\text{mm}$ and an axle with radius $r_{ax} = 1.5\text{mm}$. The width of wheels is $b = 28\text{mm}$ and projection of their center to center distance on the platform is $L_0 = 213\text{mm}$. The object is built from steel with density of $\rho = 7975\frac{kg}{m^3}$. Mass of the object is $M' = 1.618kg$ and its matrix of inertia is:

$$I = \begin{pmatrix} 0.00099 & 0 & -0.000615 \\ 0 & 0.018 & 0 \\ -0.000615 & 0 & 0.018 \end{pmatrix} \frac{kg}{m^3} \quad (50)$$

The slope of the platform is assumed to be $\beta_0 = 2.7°$. The model was built in CATIA and for dynamical analysis it was exported to MSC. ADAMS. In initial configuration, the axle is perpendicular to gradient of slope direction as it is shown in Fig. 5. The aim of simulations is to verify kinematical and dynamical equations obtained in previous sections. In the kinematics, (7) shows that the path of the object is a circle with radius *R* for small wheel and $R + L_0$ for big wheel. According to parameters of the simulated model we can obtain radius *R* from (7) as $R = 852\text{mm}$.

We simulated the system for 6 seconds in ADAMS. Fig. 8 illustrates six snapshots of the simulation. In this figure calculated target path (given by (7)) is shown by black-bold lines and the travelled path by the small wheel is shown by gray line. The center of the circle is illustrated by P.

For more accurate investigation, the curve of distance between the small wheel and the center P is shown in Fig. 9. It can be seen that the maximum deviation from the predicted path is 39.5 mm which is small deviation about 4.5% of the radius. This deviation can be originated from the simplifications made in modelling. These simplifications include neglecting of some components of the mechanism like mass and radius of the axle and also neglecting of the centrifugal force of weight of the object in *x* direction that was explained in the previous section. Interestingly the deviation before $\theta = \frac{\pi}{2}$ is very small which confirms our previous discussions. An equivalent experimental setup was also built to validate the equations and simulations (see Fig. 10).

Six snapshots of the corresponding test were shown in Fig. 11. Comparing Fig. 9 with Fig. 11 confirms matching of simulations and experiments. The deviation from the calculated path in experiments is 5.8% which is more than simulation results. This difference can be related to

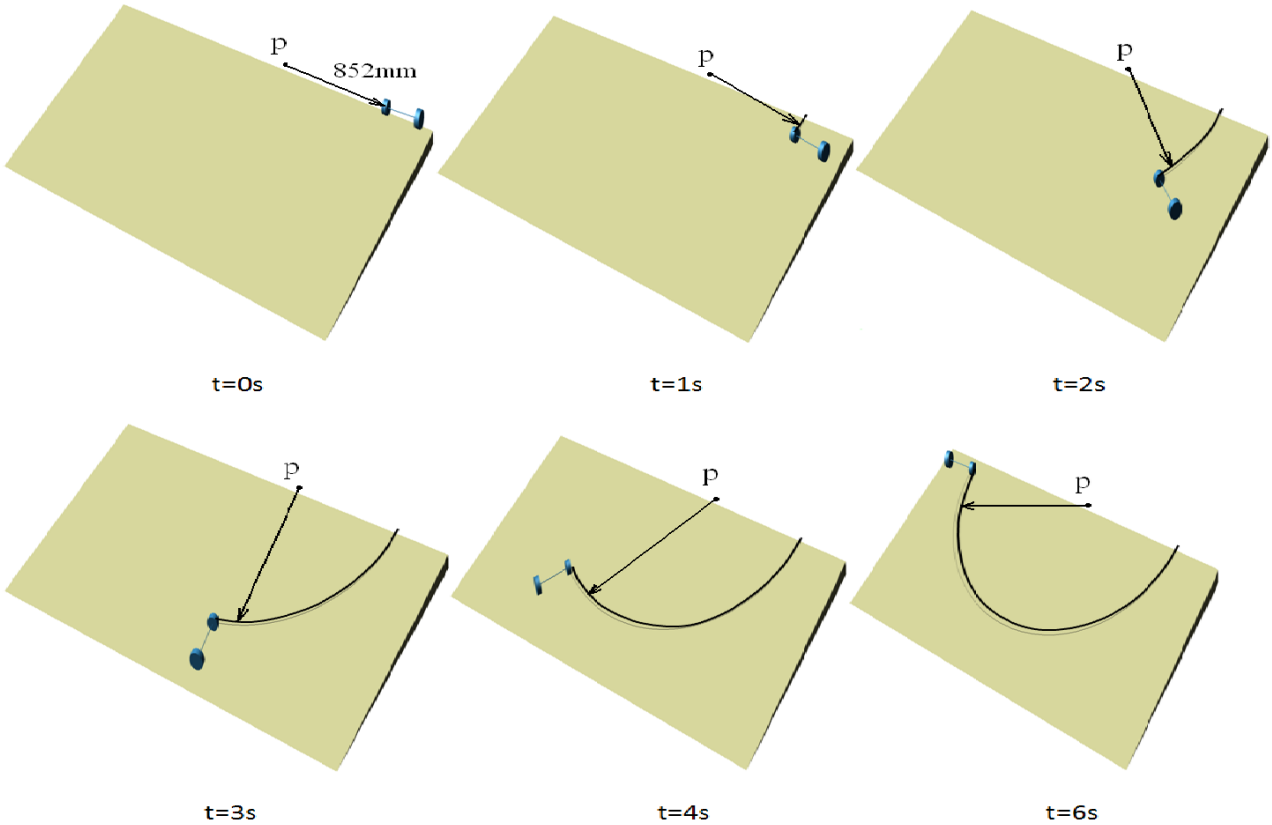

Fig. 8. Six snapshots of the simulations in ADAMS those verify that the path radius is obtained.

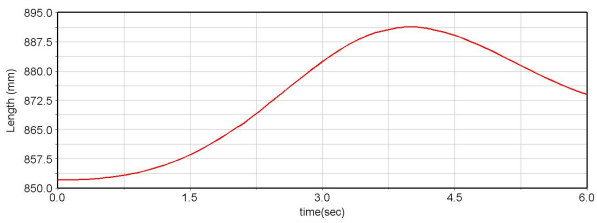

Fig. 9. Distance between the small wheel and the center of the target path (P in Fig. 7).

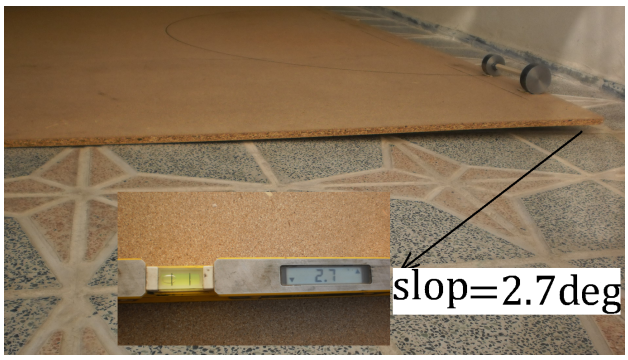

Fig. 10. Experimental setup with an object and surface with slope 2.7°

the computational inaccuracies of the software, fabrication inaccuracies of the experimental setup and slippage of the object which is not unavoidable in practice.

Above mentioned tests verify the correctness of (7) which was the outcome of the kinematical analysis. Now we are going to verify dynamical analysis that its results were summed up in (41), (42) and (43). Equations (42) and (43) are well-known equations and there is no need to verify them. These equations will be valid if linear acceleration a given by (41) is correct. Then we only need to verify (41). It should be noted that in (41), acceleration a is linear acceleration excluding centrifugal accelerations and other acceleration components. However, there is no tool in MSC.ADAMS to measure this pure linear acceleration. To resolve the issue, we consider following differential equation:

$$ads = Vdv \tag{51}$$

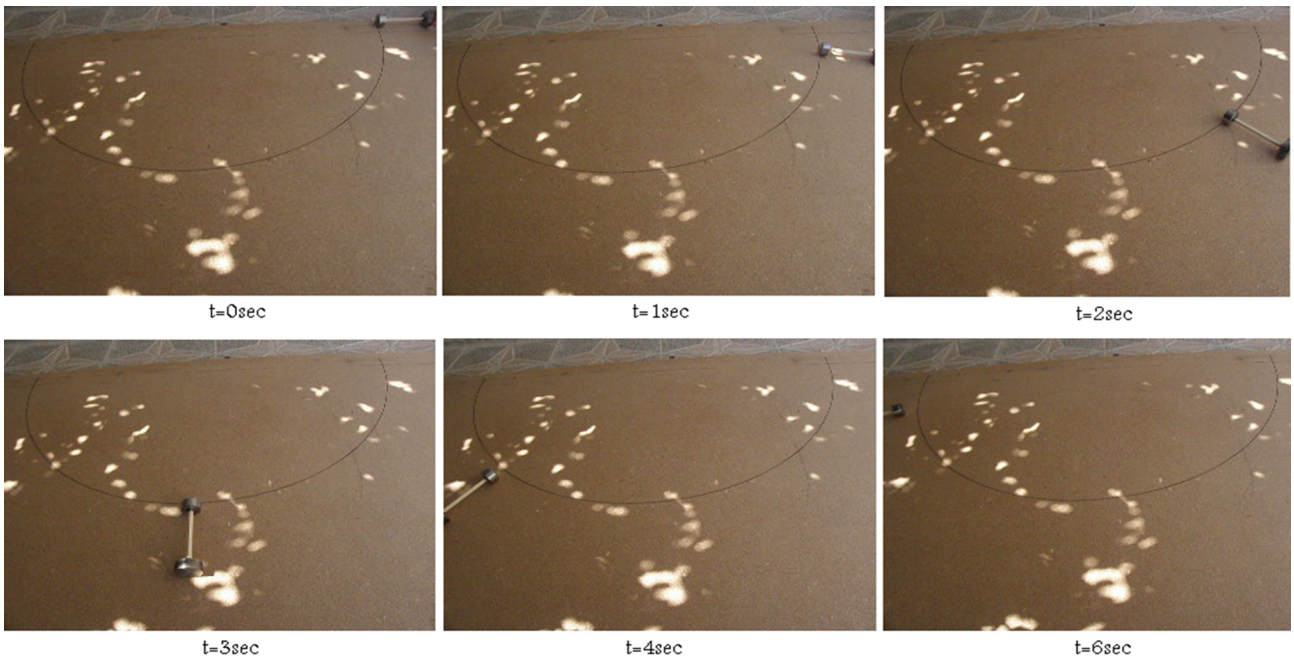

Fig. 11. Six snapshots of the experiments of proposed passive manipulation mechanism.

Substituting (41) in (51) yields:

$$\frac{(R+\bar{x})\bar{z}r_{ws}M'g\sin\beta_0}{I_{XZ}r_{ws}+I_XR+M'\bar{z}r_{ws}(R+\bar{x})}\cos\theta ds = Vdv \tag{52}$$

We define constant K as:

$$K = \frac{(R+\bar{x})\bar{z}r_{ws}M'g\sin\beta_0}{I_{XZ}r_{ws}+I_XR+M'\bar{z}r_{ws}(R+\bar{x})} \tag{53}$$

and substitute ds as $ds = Rd\theta$. Then integrating (52) with $\theta_0 = 0$ and $V_0 = 0$ yields:

$$V = \sqrt{2RK\sin\theta} \tag{54}$$

Now we can verify (54) by measuring velocity and angle of the object. Figs 12 and 13 show angle and velocity of the object during above mentioned simulation. Using data of these curves we can plot velocity in terms of angle as it is shown in Fig. 14. In Fig.14, calculated curve by (54) is depicted by blue line the result of simulations is depicted by red line. It can be seen that simulation results are near to calculated path.

5.2 Effects of the model parameters on motion

In this subsection we run some sets of simulations to study how the parameters of the mechanism affect the motion of the object. In these simulations parameters of the model are selected as the basic model presented in the previous subsection. In each simulation set, one of the characteristics of the model is changed and its influence on behavior of the mechanism is organized in a table. For each simulation set, maximum radius of the path (R_{max}), maximum deviation from the predicted path (d_{max}), percentage of deviation from predicted radius (d_{rel}) and time duration of traveling on a quarter of circular path ($t_{\pi/2}$) are provided in tables. Aforementioned simulation sets are as the following:

Table 1. The effect of slope of the surface on motion parameters. All other parameters are as basic test of subsection 5.1. Calculated radius is $R = 852$.

β_0 (degree)	R_{max} (mm)	d_{max} (mm)	d_{rel} (degree)	$t_{\frac{\pi}{2}}$ (sec)
0.9	875.254	23.254	2.729%	5.8
1.8	881.461	29.461	3.457%	4.1
2.7	891.5	39.5	4.636%	3.45
3.6	892.332	40.332	4.733%	2.932
4.5	896.907	44.907	5.27%	2.62

1. In the first set, simulations were performed with five different slopes of the surface. The results are shown in Table 1. It can be seen that bigger values of slop result in more deviation from the predicted path. This is reasonable because in higher slopes, the centrifugal force in x direction (which has been neglected in modeling) is increased. Moreover, traveling time is smaller in bigger slopes. This is also anticipated as in higher slopes vertical acceleration of the object is

Table 2. The effect of material type on motion parameters. Geometrical parameters are as basic test of subsection 5.1. Calculated radius is $R = 852$.

Material	M' (kg)	μ_s	μ_d	R_{max} (mm)	d_{max} (mm)	d_{rel} (degree)	$t_{\frac{\pi}{2}}$ (sec)
steel	1.618	0.6	0.4	881.546	29.461	3.457%	4.1
wood	0.089	0.6	0.4	890.87	38.87	4.562%	4.146
brass	1.745	0.35	0.2	885.989	33.989	3.989%	4.08
copper	1.818	0.8	0.5	880.787	28.787	3.378%	4.084

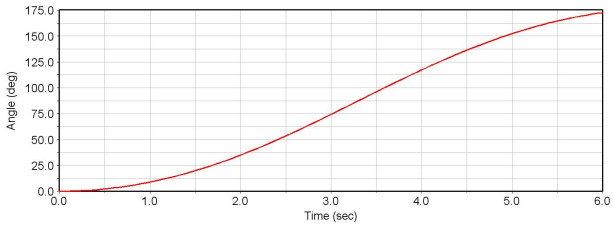

Fig. 12. Angle of the object during simulations of passive motion corresponding to Fig. 8.

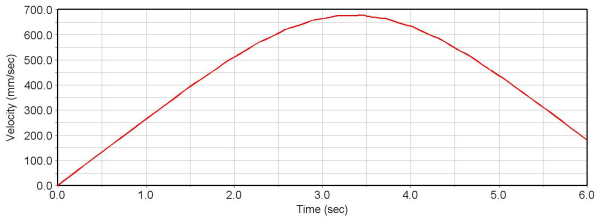

Fig. 13. Velocity of the object during simulations of passive motion corresponding to Fig. 8.

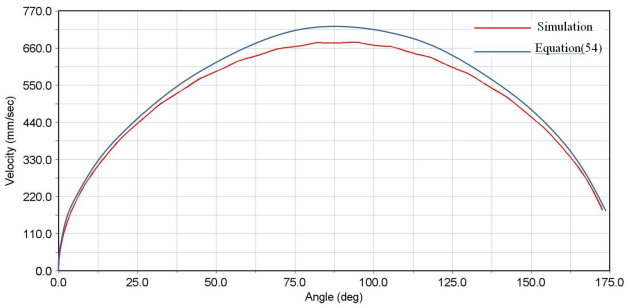

Fig. 14. Comparison of calculated path of the object given by (54) *the path obtained from simulations*

increased.

2. In the second set, the slope of the surface is fixed at 2.8° and simulations were performed with four different materials. The results are given in Table 2. For each material mass of the object and Coulomb friction coefficients are provided. By changing material type, different parameters of model namely mass and of the object and friction coefficients are changed. These parameters have diverse effects on the motion and it is not straightforward to derive an exact rule to predict effect of a specific material on motion. In general, more stiff materials have provided more deviation from the calculated path.

3. In the third set of simulations the effect of radius of small wheel with five different values for r_{sw} is investigated. As it is expected, more values of r_{sw} result in larger values of radius R. Obviously longer paths would result in larger travel times. In larger radiuses, percentage of deviation is smaller. These points show that by changing geometry of the object we can take control on motion parameters.

Table 3. The effect of radius of small wheel on motion parameters. All other parameters are as basic test of subsection 5.1.

r_{ws} (mm)	R (mm)	R_{max} (mm)	d_{max} (mm)	d_{rel} (degree)	$t_{\frac{\pi}{2}}$ (sec)
27.167	560	590.259	30.259	5.4%	3.5
28.136	640	670.568	30.568	4.776%	3.661
30	852	881.546	29.461	3.457%	4.1
30.915	1000	1029.664	29.664	2.966%	4.383
31.847	1200	1239.987	29.987	2.332%	4.8

6 CONCLUSIONS

Object manipulation has many applications in industries. One of the recently presented paradigms which is interesting from the energy saving and simplicity viewpoints is passive mechanism. Passive mechanism refers to mechanism wherein the only motion generation force is gravity force. In the passive mechanisms presented so far, generated motion have always been along a straight line. However, in many applications a straight line manipulation is not desirable. Manipulation of objects by robot arms, set of conveyors and wagons are examples where the manipulation is expected to be done in more than one dimensions.

In this paper a passive grasp-less mechanism was developed for manipulation of an object along a predictable circular path. In existing passive dynamic manipulation mechanisms a simple object has been considered and the platform has been designed to steer the object along a predefined (straight) path. Nevertheless, in this paper a different approach was selected where a simple inclined surface was considered as platform and the object is designed such that it travel along a curved path on the platform. The object is composed of two wheels with different radiuses and an axle that joins center points of the wheels (see Fig. 2).

Kinematic analysis was performed where the characteristics of object's path was obtained in terms of radiuses of wheels and length of the axle. Then dynamical analysis was provided were linear and angular accelerations of the object were obtained. The accelerations depend of geometric and inertial characteristics of the object as well as slope of the platform. Some simplifications were made in dynamic analysis in order to get a simple, applicable and understandable model as well as keeping reasonable level of accuracy. In fact a trade of was made between simplicity and accuracy of the model. Simulation and experimental results showed that the obtained model is accurate enough to describe the motion with acceptable level of accuracy.

The presented object can be used as wheels of passively driven mobile robots or vehicles. This passive mobile robot - by appropriate design - can be used in applications of Fig. 1. Designing of such a vehicle or mobile robot is future work that we are working on it.

Moreover as it was already shown in [24], [36], [37] that walking is in dynamic analogy with manipulation, this work can inspire the researchers to modify passively walking robots to change their directions during walking.

APPENDIX A

In the following we obtain different components of objects moment of inertia I. For I_X we have:

$$I_X = I_{Xwb} + I_{Xws} \tag{55}$$

where I_{Xws} and I_{Xwb} are moments of inertia of small and big wheels in X direction those can be obtained using parallel axis principle as:

$$I_{Xwb} = \bar{I}_{1wb} + m_{wb}(\bar{z}_{wb}^2 + \bar{y}_{wb}^2) \tag{56}$$

$$I_{Xws} = \bar{I}_{1ws} + m_{ws}(\bar{z}_{ws}^2 + \bar{y}_{ws}^2) \tag{57}$$

$\bar{I}_{1wb}$ and $\bar{I}_{1wS}$ are respectively the moments of inertia of the big and small wheels around their first principle axis passing in parallel to *x* and *X* through their CoG. $\bar{y}_{ws}$, $\bar{y}_{wb}$, $\bar{z}_{wb}$ and $\bar{z}_{ws}$ are z and y components of CoG of wheels in O_{XYZ} and obviously we have:

$$\bar{y}_{wb} = \bar{y}_{ws} = 0 \tag{58}$$

$$\bar{z}_{wb} = r_{wb} - \bar{z} \tag{59}$$

$$\bar{z}_{ws} = r_{ws} - \bar{z} \tag{60}$$

Substituting these values in (56) and (57) and then in (55), it yields:

$$I_X = \frac{1}{2}(m_{ws}r_{wb}^2 + m_{ws}r_{ws}^2) + m_{wb}(r_{wb} - \bar{z})^2 + m_{ws}(\bar{z} - r_{ws})^2 \tag{61}$$

We can find I_Y in similar way:

$$I_Y = I_{Ywb+}I_{Yws} \tag{62}$$

where for moments of inertia of wheels in Y direction we have:

$$I_{Ywb} = \bar{I}_{2wb} + m_{wb}(\bar{x}_{wb}^2 + \bar{z}_{wb}^2) \tag{63}$$

$$I_{Yws} = \bar{I}_{2ws} + m_{ws}(\bar{x}_{ws}^2 + \bar{z}_{ws}^2) \tag{64}$$

$\bar{I}_{2wb}$ and $\bar{I}_{2ws}$ are the moments of inertia of the wheels around their second principle axis passing in parallel to *y* and *Y* through their CoG. For *x* components of CoG of wheels in O_{XYZ} we have:

$$\bar{x}_{wb} = L_0 - \bar{x} \tag{65}$$

$$\bar{x}_{ws} = -\bar{x} \tag{66}$$

Using these relations we obtain I_Y from (62) as:

$$\begin{aligned} I_Y = {} & \tfrac{1}{12}\left(m_{wb}(3r_{wb}^2 + b^2) + m_{ws}(3r_{ws}^2 + b^2)\right) \\ & + m_{wb}\left((L_0 - \bar{x})^2 + (r_{wb} - \bar{z})^2\right) \\ & + m_{ws}\left(\bar{x}^2 + (\bar{z} - r_{ws})^2\right) \end{aligned} \tag{67}$$

Finally for I_Z we can write:

$$I_Z = I_{Zwb} + I_{Zws} \tag{68}$$

where:

$$I_{Zwb} = \bar{I}_{3wb} + m_{wb}(\bar{x}_{wb}^2 + \bar{y}_{wb}^2) \tag{69}$$

$$I_{Zws} = \bar{I}_{3ws} + m_{ws}(\bar{x}_{ws}^2 + \bar{y}_{ws}^2) \tag{70}$$

$\bar{\mathrm{I}}_{3\mathrm{wb}}$ and $\bar{\mathrm{I}}_{3\mathrm{wS}}$ are the moments of inertia of the wheels about their third principle axis passing in parallel to *z* and *Z* through their CoG. According to these relations and (68) we obtain:

$$\begin{aligned} I_Z = {} & \tfrac{1}{12}\left(m_{wb}(3r_{wb}^2 + b^2) + m_{ws}(3r_{ws}^2 + b^2)\right) \\ & + m_{wb}(L_0 - \bar{x})^2 + m_{ws}\bar{x}^2 \end{aligned} \tag{71}$$

For I_{XY} and I_{YZ}, thanks to symmetry of object we can write:

$$I_{XY} = I_{YZ} = 0 \tag{72}$$

and for I_{XZ} we have:

$$I_{XZ} = I_{XZwb} + I_{XZws} \tag{73}$$

where I_{XZwb} and I_{XZws} are products of inertia of wheels about X and Y axes and are given by:

$$I_{XZwb} = \bar{I}_{13wb} + m_{wb}\bar{x}_{wb}\bar{x}_{wb} \quad (74)$$

$$I_{XZws} = \bar{I}_{13ws} + m_{ws}\bar{x}_{ws}\bar{x}_{ws} \quad (75)$$

$\bar{I}_{13wb}$ and $\bar{I}_{13ws}$ are products of inertia of wheels about first and third axes and are zero due to symmetry of the object. Then from (73) we have:

$$I_{XZ} = m_{wb}(L_0 - \bar{x})(r_{wb} - \bar{z}) + m_{ws}\bar{x}(\bar{z} - r_{ws}) \quad (76)$$

[1] J. W. S. Chong, S. K. Ong, A. Y. C. Nee, and K. Youcef-Youmi, "Robot Programming using Augmented Reality: An interactive method for planning collision-free paths," *Robotics and Computer-Integrated Manufacturing*, vol. 25, no. 3, pp. 689-701, 2009.

[2] M. Gauthier, R. Stephane, *Robotic Micro-assembly*, John Wiley & Sons, 2011.

[3] B.Gates, "A Robot in Every Home," *Scientific American*, vol. 296, no. 1, pp. 58-65, 2007.

[4] H. Cheng, C. Heping, and L. Yong, "Object Handling using Autonomous Industrial Mobile Manipulator," In *Cyber Technology in Automation, Control and Intelligent Systems (CYBER), 2013 IEEE 3rd Annual International Conference on*, pp. 36-41, 2013.

[5] J. Sarria, M. Hector, P. Manuel, and A. Manuel, "High Speed Fragile Object Manipulation," In *ROBOT2013:* First Iberian Robotics Conference, Springer International Publishing, pp. 727-744, 2014.

[6] K. An, A. Trewyn, A. Gokhale, S. Sastry, "Model-driven performance analysis of reconfigurable conveyor systems used in material handling applications". In Proc. Cyber-Physical Systems (ICCPS), 2011 IEEE/ACM International Conference on pp. 141-150. IEEE, April 2011

[7] V. V. Protsiv, K. A. Ziborov, & S. A. Fedoriachenko, "On Formation of Kinematical and Dynamical Parameters of Output Elements of the Mine Vehicles", Scientific Bulletin of National Mining University, (4)., 2013

[8] D. Berenson, S. S. Srinivasa, & J. Kuffner, "Task space regions: A framework for pose-constrained manipulation planning." *The International Journal of Robotics Research*, doi: 10.1177/0278364910396389, 2011

[9] Xiong, Caihua, Han Ding, and You-Lun Xiong. *Fundamentals of Robotic Grasping and Fixturing*. Vol. 3. Singapore: World Scientific, 2007.

[10] C. C. Kemp, A. Edsinger, and E. Torres-Jara, "Challenges for Robot Manipulation in Human Environments," IEEE Robotics and Automation Magazine, vol. 14, no. 1, 2007.

[11] A. Saxena, J. Driemeyer, and A. Y. Ng, "Robotic Grasping of Novel Objects Using Vision," *The International Journal of Robotics Research*, vol. 27, no. 2, pp. 157-173, 2008.

[12] T. Yoshikawa, "Multifingered Robot Hands: Control for Grasping and Manipulation," *Annual Reviews in Control*, vol. 34, no. 2, pp. 199-208, 2010.

[13] S. T. Venkataraman, T. Iberall, *Dextrous Robot Hands*. Springer Publishing Company, Incorporated, 2011.

[14] B. Jeannette, A. Morales, T. Asfour, and D. Kragic, "Data-Driven Grasp Synthesis-A Survey," *IEEE Trans on Robotics*, pp. 1-21, 2013, doi: 10.1109/TRO.2013.2289018.

[15] K. Marek, J. Wyatt, and R. Stolkin, "Prediction Learning in Robotic Pushing Manipulation," In *Proceedings International Conference on Advanced Robotics*, ICAR 2009, pp. 1-6, 2009.

[16] M. J. Behrens, "Robotic Manipulation by Pushing at a Single Point with Constant Velocity: Modeling and Techniques," PhD thesis, University of Technology, Sydney, 2013.

[17] E. Yoshida, M. Poirier, J. P. Laumond, O. Kanoun, F. Lamiraux, R. Alami, and Y. Kazuhito, "Pivoting based Manipulation by a Humanoid Robot," *Autonomous Robots*, vol. 28, no. 1, pp. 77-88, 2010.

[18] T. H. Vose, P. Umbanhowar, K. M. Lynch, "Sliding Manipulation of Rigid Bodies on a Controlled 6-DoF Plate," *The International Journal of Robotics Research*, vol. 31, no. 7, pp. 819-838, 2012.

[19] A. Akbarimajd, M. Nili Ahmadabadi, "Manipulation by Juggling of Planar Polygonal objects Using Tow 3–DOF Manipulators," *IEEE/ASME conf, on Advenced Intelligent Mechatronics* (AIM), (Zurich), sept 2007.

[20] A. Akbarimajd, "Optimal Motion Planning of Juggling by 3-DOF Manipulators using Adaptive PSO Algorithm," *Robotica*, 2014, doi:10.1017/S026357471300115X

[21] G. Batz,, A. Yaqub, H. Wu, K. Kuhnlenz, D. Wollherr, & M. Buss, "Dynamic manipulation: Nonprehensile ball catching". In Proc. Control & Automation (MED), 2010 18th Mediterranean Conference on (pp. 365-370). IEEE., June 2010

[22] T. Kizaki, and A. Namiki, "Two Ball Juggling with High-speed Hand-arm and High-speed Vision System," *In proceedings of International Conference on Robotics and Automation* (ICRA), pp. 1372-1377, 2012.

[23] M. Higashimori, K. Utsumi, Y. Omoto, & M. Kaneko, M., Dynamic manipulation inspired by the handling of a pizza peel. *Robotics, IEEE Transactions on*, *25*(4), 829-838, 2009

[24] I. G. Ramirez-Alpizar, M. Higashimori, M. Kaneko, C. H. Tsai, & I. Kao, "Dynamic Nonprehensile Manipulation for Rotating a Thin Deformable Object: An Analogy to Bipedal Gaits" Robotics, IEEE Transactions on, 28(3), 607-618., 2012

[25] A. Bicchi, K. T. Goldberg, "Minimalism in Robot Manipulation," in *lecture Notes, Workshop in 1966 IEEE international conference on Robotics and Automation*, 1996.

[26] S. Akellas, W.H. Huang, K. M. Lynch, and M. T. Mason, "Parts Feeding on a Conveyor with a one Joint Robot," *Journal of Algorithmica*, vol. 26, pp. 313 – 344. 2000.

[27] A. Akbarimajd, M. Nili AhmadAbadi, B. Beigzadeh, "Dynamic Object Manipulation by an Array of 1-DOF Manipulators: Kinematic Modeling and Planning," *Robotics and Autonomous System*, vol. 55, No. 6, pp. 444-459, 2007.

[28] T. Mcgeer, "Passive Dynamic Walking," *International Journal of Robotics Research*, vol. 7, no. 2, pp. 62 – 82, 1990.

[29] S. Collins, A. Ruina, R. Tedrake, and M. Wisse, "Efficient Bipedal Robots Based on Passive-Dynamic Walkers," *Science*, vol. 307, no. 5712, pp. 1082-1085, 2005.

[30] M.W. Spong, and F. Bullo, "Controlled Symmetries and Passive Walking," *IEEE Transactions on Automatic Control*, vol. 50, no. 7, pp. 1025-1031, 2005.

[31] Y. Ikemata, A. Sano, and H. Fujimoto, "Generation and Local Stabilization of Fixed Point Based on a Stability Mechanism of Passive Walking," In *Proceedings 2007 IEEE International Conference on Robotics and Automation*, pp. 3218-3223, 2007.

[32] F. Asano, Z. W. Luo, "Asymptotically Stable Biped Gait Generation Based on Stability Principle of Rimless Wheel," *Robotica*, vol. 27, no. 6, 2009.

[33] J. S. Moon, M. W. Spong, "Bifurcations and Chaos in Passive Walking of a Compass-gait Biped with Asymmetries," In *Proc. 2010 IEEE International Conference on Robotics and Automation* (ICRA), pp. 1721-1726, 2010.

[34] J. S. Moon, M. W. Spong, "Energy plane analysis for passive dynamic walking," In *Proc. 12th IEEE-RAS International Conference on Humanoid Robots* (Humanoids), pp. 580-585, 2012.

[35] K. Rushdi, D. Koop, and C. Q. Wu, "Experimental Studies on Passive Dynamic Bipedal Walking," *Robotics and Autonomous Systems*, 2013, doi: 10.1016/j.robot.2013.12.002.

[36] B. Beigzadeh, M. Nili Ahmadabadi, A. Meghdari, and A. Akbarimajd, "A Dynamic Object Manipulation Approach to Dynamic Biped Locomotion," *Robotics and Autonomous Systems* vol. 56, no. 7, pp. 570-582, 2008.

[37] A. Akbarimajd, M. Nili Ahmadabadi, and A. Ijspeert, "Analogy between Juggling and Hopping: Active object manipulation approach," *Advanced Robotics*, vol. 25, no. 13-14, pp. 1793-1816, 2011.

[38] B. Beigzadeh, A. Megdari, S. Sohrabpour, "Passive Dynamic Object Manipulation: Preliminary Definition and Examples," *Acta Automatica Sinica*, vol. 36, no 12, pp. 1711-1719, 2010.

[39] A. Bajelan, A. Akbarimajd, "A New Non-Actuated Mechanism for Nonprehensile Object Manipulation," In *Proc. In conf on 3rd International Conference on Automation, Robotics and Mechanical Engineering*, (Dubai), 2014.

Abdullah Bajelan

received his B.Sc. degree in Mechanical Engineering from Kar University of Rafsanjan, Iran in 2011. Then he entered University of Mohaghegh Ardabili, Ardabil, Iran as M. Sc. Student in mechanical engineering. His research interests include mechanism design, dynamics and robotics.

Adel Akbarimajd

received his B.Sc. degree in Control Engineering from Ferdowsi University of Mashhad, Iran in 1997 and M.S. degree in Control Systems from Tabriz University of Iran in 2000. In 2007, he spent six month in the Biorobotics Laboratory, EPFL, Switzerland as visiting researcher in the framework of biped legged locomotion. He received his Ph.D. in AI and robotics from university of Tehran in 2009. Later he moved to Department of Engineering at University of Mohaghegh Ardabili, where he currently is an associate professor. He has been head of electrical and computer engineering department at University of Mohaghegh Ardabili since 2011. His research interests include robot manipulation more specifically dynamic object manipulation, legged robots with focus on biped and monopod locomotion, bio-inspired locomotion mechanisms and finally planning and control of mobile robots.

AUTHORS' ADDRESSES

Abdullah Bajelan, B.Sc.,
Assoc. Prof. Adel Akbarimajd, Ph.D.,
Faculty of Technical Engineering,
University of Mohaghegh Ardabili,
Ardabil, Iran,
email: abdoallah.bajelan@yahoo.com
akbarimajd@gmail.com

Received: 2014-03-23
Accepted: 2015-01-27